Sixth International Symposium on Turbulence and Shear Flow Phenomena
Seoul, Korea, 22-24 June 2009

FURTHER INSIGHT INTO SUBGRID-SCALE TRANSPORT MODELING FOR CONTINUOUS HYBRID RANS/LES FLOW SIMULATIONS

Bruno Chaouat
Department of Computational Fluid Dynamics, ONERA
BP 72 - 92322 Châtillon cedex, France
Bruno.Chaouat@onera.fr

Roland Schiestel
IRPHE CNRS/Universités d'Aix-Marseille I & II
Technopôle Château-Gombert, BP 146 - 13384 Marseille cedex 13, France

ABSTRACT

The partially integrated transport modeling (PITM) method viewed as a continuous approach of hybrid RANS/LES with seamless coupling is presented. It is used for deriving a subgrid stress model based on the subgrid stresses and the dissipation rate developed in a general formulation for free flows as well as bounded flows. This model is then applied for predicting the well know turbulent channel flow as well as the periodic flow over a 2d hill which presents complex physics. As a result, it is found that the subgrid scale stress model is able to simulate the flows performed on coarse grids with satisfactory agreements with the reference data for both the velocity and the turbulent stresses and provides the detail of the flow structures.

INTRODUCTION

Mathematical turbulence modeling methods such as Reynolds averaged Navier-Stokes methods or large eddy simulations methods (Schiestel, 2007) have been proposed independently each other for simulating turbulent flows. Generally, advanced RANS models such as Reynolds Stress Models (RSM) (Launder, 1989) appear well suited for tackling engineering flows encountered in aeronautical applications (Hanjalic and Jakirlic, 1998; Chaouat, 2005; Gatski, 2007) whereas subgrid-scale models used in LES such the dynamic model or structure model (Lesieur et al., 1996) are rather considered for simulating academic flows with emphasis on fundamental aspects and structural aspects. Although these methods are very useful, each of them has its own specific field of application. Statistical RANS models are not well suited for studying unsteady flows subjected to a large range of frequencies that can interact with the turbulence time scales. On the other hand, large eddy simulations are not accurate when they are performed on coarse grids since the subgrid-scale energy is generally modeled by a simple closure only valid for fine grained turbulence and require very large computing times. For these reasons, hybrid RANS/LES zonal methods, capable of reproducing a RANS-type behavior in the vicinity of a solid boundary and an LES-type behavior far away from the wall boundary have been developed in the last decade (Spalart, 2000; Hanjalic and Kenjeres, 2008). They rely on two different models, statistical and subgrid models that are applied in different domains separated by an interface. Although of practical used for aeronautical applications, the interface poses matching problems between the RANS and LES regions.

Recently, the partially integrated transport modeling (PITM) method has been proposed (Chaouat and Schiestel, 2005; Schiestel and Dejoan, 2005) to overcome these difficulties. This method allows to perform hybrid non-zonal RANS/LES simulations on relatively coarse grids with seamless coupling and bridges two different levels of description in a consistent way based on the spectral theoretical PITM methodology (Chaouat and Schiestel, 2007). Thus, it gains major interest on the fundamental point of view because it allows some unifying formalism that conciliates RANS and LES approaches.

The paper presents briefly the PITM method and describes numerical flow simulations using the subgrid scale stress model developed in a general formulation for free flows as well as bounded flows (Chaouat and Schiestel, 2009). The fully developed turbulent channel flow is first simulated on two different meshes for checking the grid independence of the solutions as well as the consistency of the subgrid-scale model when the filter width is changed. The second simulation is concerned with a periodic flow over a 2d hill (Fröhlich et al.,2005). This test case is of central interest because of the turbulence mechanisms associated with separation, recirculation, reattachment, acceleration and wall flow effects that are difficult to reproduce. Comparisons of the results are made with highly resolved LES using the dynamic Smagorinsky model (Fröhlich et al., 2005; Breuer et al., 2009).

THE FILTERING PROCESS AND TRANSPORT EQUATION SUBFILTER MODEL

The governing equations

Turbulent flow of a viscous incompressible fluid is considered. In large eddy simulations, the flow variable ϕ is decomposed into a large scale (or resolved) part $\bar{\phi}$ and a subgrid-scale fluctuating part ϕ'. The large scale component is defined by the filter function G_Δ as

$$\bar{\Phi}(x_i) = \iiint_{\mathcal{D}} \prod_{i=1}^{3} G_{\Delta_i}(x_i, x_i')\, \Phi(x_1', x_2', x_3')\, d^3x_i' \qquad (1)$$

where Δ_i is the filter width in the i-direction. Applying the filtering operation to the continuity and Navier-Stokes

equations yields the filtered momentum equations

$$\frac{\partial \bar{u}_i}{\partial t} + \frac{\partial}{\partial x_j}\left(\bar{u}_i \bar{u}_j\right) = -\frac{1}{\rho}\frac{\partial \bar{p}}{\partial x_i} + \nu \frac{\partial^2 \bar{u}_i}{\partial x_j \partial x_j} - \frac{\partial (\tau_{ij})_{sgs}}{\partial x_j} \quad (2)$$

where u_i, p, $(\tau_{ij})_{sgs}$, are the velocity vector, the pressure, and the subgrid-scale stress tensor. The subgrid-scale tensor $(\tau_{ij})_{sgs}$ is defined by the mathematical relation

$$(\tau_{ij})_{sgs} = \overline{u_i u_j} - \bar{u}_i \bar{u}_j \quad (3)$$

The presence of the turbulent contribution $(\tau_{ij})_{sgs}$ in equation (2) indicates the effect of the subgrid scales to the resolved field. The resolved scale tensor is defined by the relation

$$(\tau_{ij})_{les} = \bar{u}_i \bar{u}_j - \langle u_i \rangle \langle u_j \rangle \quad (4)$$

where $\langle . \rangle$ denotes the statistical average. So that, the Reynolds stress tensor τ_{ij} including the small and large scale fluctuating velocities is computed by the sum of the subgrid and resolved stresses

$$\tau_{ij} = \langle (\tau_{ij})_{sgs} \rangle + \langle (\tau_{ij})_{les} \rangle \quad (5)$$

whereas the statistical turbulent energy is obtained as the half-trace of equation (5) leading to $k = \langle k_{sgs} \rangle + \langle k_{les} \rangle$.

The subgrid-scale stress model

The subgrid scale stress modeling finds its basic foundation in the spectral space by considering the Fourier transform of the two-point fluctuating velocity correlation equations in homogeneous turbulence (Chaouat and Schiestel, 2007). The extension to non-homogeneous turbulence is developed within the framework of the tangent homogeneous space. From a physical point of view, it is assumed in the LES framework that the interaction mechanisms of the subgrid-scales with the resolved scales of the turbulence are of the same nature than the interaction mechanisms involving all the fluctuating scales with the mean flow, allowing transposition of closure hypotheses from RANS to LES. As a result of the modeling, the subgrid-scale model based on the transport equations for the subgrid-scale stresses $(\tau_{ij})_{sgs}$ and the subgrid dissipation rate ϵ_{sgs} look formally like the corresponding RANS/RSM model but the coefficients used in the model are no longer constants. They are now some functions of the dimensionless parameter η_c involving the cutoff wave number κ_c and of the turbulent length scale L_e built using the total turbulent kinetic energy $k = \langle k_{sgs} \rangle + \langle k_{les} \rangle$, the total dissipation rate $\epsilon = \langle \epsilon_{sgs} \rangle + \langle \epsilon^< \rangle$ composed of the subgrid dissipation rate ϵ_{sgs} and the macro-scale dissipation rate $\epsilon^<$

$$\eta_c = \kappa_c L_e = \frac{\pi\, k^{3/2}}{(\Delta_1 \Delta_2 \Delta_3)^{1/3}\ \epsilon} \quad (6)$$

The main feature of the PITM method is that the subgrid-scale stress model varies now continuously with respect to the ratio of the turbulent length-scale to the grid-size L_e/Δ. For the limiting condition when the parameter η_c goes to zero, the subgrid-scale model behaves like a RANS/RSM model whereas when η_c goes to infinity, the computation switches to DNS or under resolved DNS if the grid-size is not enough refined because the energy cannot be maintained. In regard with academic LES simulations which require that the spectral cutoff must be located within the inertial range, the present subgrid-scale stress model allows to perform flow simulations on relatively coarse grids since the cutoff wavenumber can be located almost anywhere inside the spectrum. By using the material derivative operator $D/Dt = \partial/\partial t + \bar{u}_k \partial/\partial x_k$, the transport equation of the subgrid stress tensor can be written in the simple compact form as

$$\frac{D(\tau_{ij})_{sgs}}{Dt} = P_{ij} + \Psi_{ij} + J_{ij} - (\epsilon_{ij})_{sgs} \quad (7)$$

where the terms appearing in the right-hand side of this equation are identified as production, redistribution, diffusion and dissipation. The production term P_{ij} is produced by the interaction between the subgrid stress and the filtered gradient velocity

$$P_{ij} = -(\tau_{ik})_{sgs}\frac{\partial \bar{u}_j}{\partial x_k} - (\tau_{jk})_{sgs}\frac{\partial \bar{u}_i}{\partial x_k} \quad (8)$$

The redistribution, diffusion and dissipation terms need to be modeled. Like in RANS modeling, the redistribution term Ψ_{ij} is decomposed into a slow part Ψ^1_{ij} and a rapid part Ψ^2_{ij}. The slow term Ψ^1_{ij} characterizes the return to isotropy due to the action of turbulence on itself whereas the rapid term Ψ^2_{ij} describes the return to isotropy by action of the filtered velocity gradient The term Ψ^1_{ij} is modeled assuming that the usual statistical Reynolds stress models must be recovered in the limit of vanishing cutoff wave number κ_c and considering also that the small scales return more rapidly to isotropy than the large scales before cascading into smaller scales by non-linear interactions

$$\Psi^1_{ij} = -c_{sgs_1}\frac{\epsilon_{sgs}}{k_{sgs}}\left((\tau_{ij})_{sgs} - \frac{2}{3}k_{sgs}\,\delta_{ij}\right) \quad (9)$$

where c_{sgs_1} is an increasing function of the parameter η_c and the second term Ψ^2_{ij} is modeled by

$$\Psi^2_{ij} = -c_2\left(P_{ij} - \frac{1}{3}P_{mm}\,\delta_{ij}\right) \quad (10)$$

where the coefficient c_2 remains the same than in statistical modeling. The diffusion term J_{ij} appearing in equation (7) due to the fluctuating velocities and pressure together with the molecular diffusion, is modeled assuming a gradient law hypothesis

$$J_{ij} = \frac{\partial}{\partial x_k}\left(\nu\frac{\partial (\tau_{ij})_{sgs}}{\partial x_k} + c_s\frac{k_{sgs}}{\epsilon_{sgs}}(\tau_{kl})_{sgs}\frac{\partial (\tau_{ij})_{sgs}}{\partial x_l}\right) \quad (11)$$

where c_s is a numerical coefficient set to 0.22. Closure of equation (7) needs to model the subgrid tensorial dissipation rate $(\epsilon_{ij})_{sgs}$ which is approached by $2/3\epsilon\delta_{ij}$. The modeling of dissipation-rate ϵ_{sgs} is made in the present case by means of its transport equation. This allows to obtain an accurate estimate of the subgrid dissipation rate even in situation of non-equilibrium flows when the grid-size is no longer a good estimate of the characteristic turbulence length-scale. As a result of the theory developed in the spectral space (Chaouat and Schiestel, 2007), the fluctuating modeled transport equation for the subgrid-scale dissipation-rate ϵ_{sgs} reads

$$\frac{D\epsilon_{sgs}}{Dt} = c_{sgs\epsilon_1}\frac{\epsilon_{sgs}}{k_{sgs}}P - c_{sgs\epsilon_2}\frac{\epsilon^2_{sgs}}{k_{sgs}} + J_\epsilon \quad (12)$$

where $P = P_{mm}/2$. The coefficient $c_{sgs\epsilon_1}$ is constant whereas the coefficient $c_{sgs\epsilon_2}$ appearing in equation (12) is now a function of the ratio to the subgrid energy to the total energy $\langle k_{sgs} \rangle / k$ as follows (Chaouat and Schiestel, 2007)

$$c_{sgs\epsilon_2} = c_{\epsilon_1} + \frac{\langle k_{sgs} \rangle}{k}\left(c_{\epsilon_2} - c_{\epsilon_1}\right) \quad (13)$$

and where the coefficients c_{ϵ_1} and c_{ϵ_2} appearing in this equation denote the usual constants used in the statistical dissipation rate transport equation. The theory shows that the coefficients of the production term remain the same for both RANS and LES dissipation-rate equations $c_{sgs\epsilon_1} = c_{\epsilon_1} = 3/2$. In the present case, the values retained are $c_{\epsilon_1} = 1.45$ and $c_{\epsilon_2} = 1.9$. Equation (12) using the relation (13) constitutes the main feature of the PITM approach where only the part of the spectrum for $\kappa > \kappa_c$ is modeled. The ratio k_{sgs}/k appearing in equation (13) is evaluated by means of an accurate energy spectrum $E(\kappa)$ inspired from a Von Kármán like spectrum valid on the entire range of wavenumbers leading to the result (Chaouat and Schiestel, 2009)

$$c_{sgs\epsilon_2}(\eta_c) = c_{\epsilon_1} + \frac{c_{\epsilon_2} - c_{\epsilon_1}}{[1 + \beta_\eta\, \eta_c^3]^{2/9}} \qquad (14)$$

Equation (14) indicates that the function $c_{sgs\epsilon_2}$ acts like a dynamical parameter which controls the spectral distribution of turbulence and verifies the limiting behaviors $lim\ _{\eta_c \to 0}\ c_{sgs\epsilon_2}(\eta_c) = c_{\epsilon_2}$, implying that the model behaves like a RANS/RSM whereas $lim\ _{\eta_c \to \infty} c_{sgs\epsilon_2}(\eta_c) = c_{\epsilon_1}$ meaning that the computation switches to DNS (or under resolved DNS if the grid-size is not enough refined) because the subgrid-energy can not maintain. The theoretical value of the coefficient β_η in equation (14) is $\beta_{\eta_\mathcal{T}} = (2/3C_K)^{9/2}$ where C_K is the Kolmogorov constant. In practice, this value is optimized for $C_K = 1.3$ according to previous flow simulations. The diffusion term J_ϵ appearing on the left hand side of equation (12) is modeled assuming a well-known gradient law hypothesis

$$J_\epsilon = \frac{\partial}{\partial x_j}\left(\nu \frac{\partial \epsilon_{sgs}}{\partial x_j} + c_\epsilon \frac{k_{sgs}}{\epsilon_{sgs}} (\tau_{jm})_{sgs} \frac{\partial \epsilon_{sgs}}{\partial x_m}\right) \qquad (15)$$

where the coefficient c_ϵ is set to 0.18.

NUMERICAL METHOD AND CONDITIONS OF COMPUTATIONS

Numerical method

The numerical simulations are performed using a research code (Chaouat, 2009) which is based on a finite volume technique. The governing equations of motion as well as the transport equations of the stresses and dissipation-rate are integrated in time by a Runge-Kutta scheme of fourth-order accuracy. The convective fluxes at the interfaces resulting from the finite volume technique are computed by a numerical scheme of second-order accuracy in space which is based on a quasi-centered discretized formulation of the flow variables. The source terms of the turbulent equations are solved by an implicit scheme to improve the numerical stability. The code has been successfully calibrated on the decay of homogeneous isotropic turbulence and fully turbulent channel flows. Since the present hybrid RANS/LES simulations require less grid points in the streamwise and spanwise directions than in the normal direction, the CPU time consuming is reduced in regard with refined LES simulations, although more equations need to be solved at each time advancement.

NUMERICAL FLOW SIMULATIONS

Fully turbulent channel flow

The test case of the fully developed turbulent channel flow is considered for analyzing the potentials of the subgrid-stress model regarding its capacity to reproduce the flow anisotropy and wall flows. Two different meshes are generated with a coarse and a medium spatial resolutions $16 \times 32 \times 64$ and $32 \times 64 \times 84$, respectively in the streamwise, spanwise and normal directions for checking the grid independence of the solutions. The dimensions of the channel are $2\delta \times 2\delta \times \delta$. In the normal direction to the wall, the grid points are distributed using non-uniform spacing with refinement near the wall whereas they are uniform in the two remaining directions, $\Delta_1^+ = 105.3$, $\Delta_2^+ = 50.9$ for case 1 and $\Delta_1^+ = 50.9$, $\Delta_2^+ = 25.1$ for case 2. The LES results are compared with DNS (Moser et al, 1999) for a Reynolds number $R_\tau = 395$, based on the friction velocity u_τ and the channel half width $\delta/2$. For comparison purposes, numerical LES simulations using the Smagorinsky model in a version proposed by Lilly are also performed. Figure 1 shows the profiles of the statistical mean velocity $\langle u_1 \rangle / u_\tau$ for both simulations that agree well with DNS data. Figure 2 displays the evolutions of the subgrid and resolved stresses in the streamwise, spanwise and normal direction, respectively, for the coarse and refined meshes. One can see that the subgrid scale stresses are indeed anisotropic in the vicinity of the walls and that the sharing out of the turbulence energies is governed by the grid size. Figure 3 describes the evolutions of the normalized total Reynolds stresses for the two LES simulations performed on the coarse and refined meshes It appears that the subgrid stresses agree well with the DNS data for both the coarse and refined grids but the stresses computed on the coarse mesh by the Smagorinsky model highly overpredict the DNS data. Figure 4 concerned with the budget of the subgrid turbulent energy shows the evolutions of the subgrid production, diffusion and dissipation terms P_{sgs}, J_{sgs}, ϵ_{sgs} in logarithmic coordinate for the coarse LES simulation. Since these terms become important close to the wall and decrease rapidly away the wall, it is clear that the grid must be sufficiently refined near the walls for correctly reproducing the physical processes acting in the boundary layer, even when simulating industrial flows. The two-point correlations of the resolved scales located on the centerline of the channel $x_3 = \delta$ are plotted on figure 5. As expected, the box size is adequate since the longitudinal two-point correlation tensor almost returns to zero and it is found that the velocity correlation R_{11} in the streamwise direction is larger than the corresponding transverse correlations R_{22} or R_{33}. It is remarkable however that the present calculation, in spite of its coarse grid resolution in the center of the channel, succeeded in providing a good qualitative evolution of the two-point correlation tensor.

Channel flow with streamwise periodic constrictions

The simulation of a periodic flow over a 2d hill is performed on a coarse mesh in the aim to illustrate the potentials of the PITM method, compared to RANS/RSM simulations. In particular, this test case is considered because of the turbulence mechanisms associated with separation, recirculation, reattachment, acceleration and wall flow effects that are difficult to reproduce. The hills constricts the channel by about one third of its height and are spaced at a distance of about 9 hill heights as seen in figure 6. The dimension of the computational domain are $L_1 = 9h$, $L_2 = 4.5h$ and $L_3 = 3.036h$, where h denotes the hill height, respectively in the streamwise, spanwise and normal directions. The Reynolds number, based on the hill height and the bulk velocity about the crest is 10595. This flow was previously investigated by large-eddy simulation (Fröhlich et al., 2005; Breuer et al., 2009) using a dynamic Smagorinsky model on refined meshes of about 4.6 and 13.1 million

grid points. In the present case, numerical simulations are performed on a coarse curvilinear mesh $80 \times 30 \times 100$ in the streamwise, spanwise and normal directions (1/4 million grid points) as shown in figure 6, using a RSM model (Chaouat, 2006) and the PITM subgrid-scale stress. The grid is however refined in the wall region for providing a full resolution of the boundary layer without requiring wall functions. Note that other team (Jakirlic et al., 2009) also performed this case using a variant PITM model. Concerning the computational domain, a no-slip and impermeability boundary conditions are used at the wall whereas periodic conditions are applied in the streamwise and spanwise directions. A mean pressure gradient term is included in the momentum equation for balancing the viscous friction at the walls. In practice, the coeficient C_k appearing in the coefficient β_η has been set to 1.4 to obtain an appreciable part of the subgrid energy in comparison with the resolved energy. Several numerical attempts have also revealed that equation (6) provides a too strong coupling with equations (7) and (12). In the following, the computed results are compared with highly resolved large-eddy simulation (Breuer et al., 2009). Figure 7 shows the streamlines of the instantaneous flow field performed on the coarse grid by the PITM model. The recirculation zone that extends in the lower wall region is well visible. Figure 8 displays the velocity profiles at three locations $x/h = 2, 4, 6$ and reveals a good agreement with the reference data for both the RSM and PITM computations. It appears however that the RSM velocities disagree with the data in the immediate vicinity of the lower wall regions and indicated that the flow reattaches too early in the downstream channel. This difference should probably attributed to the three dimensional flow effects that cannot be reproduced by a RANS computation because of the 2d-geometry. Figure 9, 10, and 11 show the evolutions of the turbulent energy, the streamwise turbulent energy and the turbulent shear stress, respectively, at the three locations $x/h = 2, 4, 6$ for both the RSM and PITM computations. In comparison with the highly resolved LES, one can see that the turbulent intensity of the flow is well reproduced by the RSM and PITM models. In particular, the stress profiles present a qualitative good agreement with refined LES although some discrepancies can be observed in the lower wall region. The PITM computation slightly underpredicts the turbulence intensity in the core flow whereas the RSM model returns a lower turbulent peak in the upper wall region. At this step, it seems also that the statistical convergence is not fully reached since the PITM profiles are not perfectly regular as it could be expected. This suggests that more temporal iterations must be run to achieve a full statistical convergence.

CONCLUSION

The PITM approach viewed as a continuous hybrid RANS/LES model has been successfully applied for simulating internal flows. The performance of the model and especially, its capabilities in the anisotropy prediction have been demonstrated in the fully turbulent channel flow test case. The subgrid stress model has also fairly well reproduced the complex physics of the separated flow in the channel with streamwise periodic constrictions, allowing also a drastic saving of the computational time because of the coarse mesh resolution. So that, it looks as a good candidate for simulating turbulent flows that presents complex physics, providing the numerical scheme is sufficiently stable and accurate.

REFERENCES

Breuer, M., Peller, N. Rapp, C. and Manhart, M., 2009, "Flow Over Periodic hills - Numerical and Experimental Study in a Wide Range of Reynolds Numbers", *Computers and Fluids*, Vol. 38, pp. 433-457.

Chaouat, B., and Schiestel, R., 2005, "A New Partially Integrated Transport Model for Subgrid-Scale Stresses and Dissipation Rate for Turbulent Developing Flows", *Physics of Fluids*, Vol. 17, n°6, 065106.

Chaouat, B., 2007, "Reynolds Stress Transport Modeling for High-Lift Airfoil Flows", *AIAA Journal*, Vol. 44, n°10, pp. 2390-2403.

Chaouat, B., and Schiestel, R., 2007, "From Single-Scale Turbulence Models to Multiple-Scale and Subgrid-Scale Models by Fourier Transform", *Theoretical and Computational Fluid Dynamics*, Vol. 21, n°3, pp. 201-229.

Chaouat, B., and Schiestel, R., 2009, "Progress in Subgrid-Scale Transport for Continuous Hybrid Non-Zonal RANS/LES Simulations *International Journal of Heat and Fluid Flow.*

Chaouat, B., 2009, "A Numerical Method for RANS and Hybrid RANS/LES Simulations of Compressible Flows Using Stress Transport Turbulence Modeling" *Submitted to Computers and Fluids.*

Fröhlich, J., Mellen, C., Rodi, W., Temmerman, L. and Leschziner, M., 2005, "Highly Resolved Large-Eddy Simulation of Separated Flow in a Channel with Streamwise Periodic Constriction", *Journal of Fluid Mechanics*, Vol. 526, pp. 19-65.

Gatski, T. B., Rumsey, C. and Manceau, R., 2007, " Current Trends in Modelling Research for Turbulent Aerodynamic Flows", *Phil. Trans. Royal Society*, Vol. 365, pp. 2389-2418.

Hanjalic, K. and Jakirlic, S., 1998, "Contribution Towards the Second-Moment Closure Modeling of Separating Turbulent Flows", *Computers and Fluids*, Vol. 27, pp.137-156.

Hanjalic, K. and Kenjeres, S., 2008, "Some developments in turbulence modeling for wind and environmental engineering", *Journal of Wind Engineering and Industrial Aerodynamics*, Vol. 96, pp.1537-1570.

Jakirlic, S., Saric, S., Kadavelil, G., Sibubalo, E., Basara, B. and B. Chaouat, 2009, "SGS Modeling in LES of Wall-Bounded Flows Using SMC and Related RANS Closures: Towards a Seamless Hybrid LES/RANS Method", 6^{th} *International Symposium and Shear Flow Phenomena.*

Launder, B. E., and Shima, N., 1989, "Second Moment Closure for the Near Wall Sublayer: Development and Application", *AIAA Journal*, Vol. 27, pp. 1319-1325.

Lesieur, M., and Metais, O., 1996, "New Trends in Large-eddy Simulations of Turbulence", *Ann. Rev Journal of Fluid Mechanics*, Vol. 28, pp. 45-82.

Moser, R., Kim, D., and Mansour, N, 1999, "Direct Numerical Simulation of Turbulent Channel Flow up to $R_\tau = 590$", *Physics of Fluids*, Vol. 11, pp. 943-945.

Schiestel, R., and Dejoan, A., 2005, "Towards a New Partially Integrated Transport Model for Coarse Grid and Unsteady Turbulent Flow Simulations", *Theoretical and Computational Fluid Dynamics*, Vol. 18, pp. 443-468.

Schiestel, R., 2008, "Modeling and Simulation of Turbulent Flows", *ISTE Ltd and J. Wiley.*

Spalart, P. R., 2000," Strategies for turbulence modelling and simulations", *International Journal of Heat and Fluid Flow*, Vol. 21, pp. 252-263.

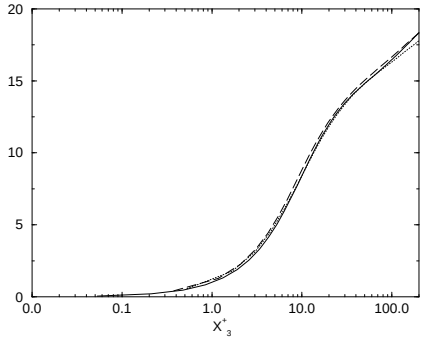

Figure 1: Fig. 1. Mean velocity profile; $\langle u_1 \rangle / u_\tau$ LES 1 ($16 \times 32 \times 64$) ...; LES 2 ($32 \times 64 \times 84$) - -; DNS —; $R_\tau = 395$.

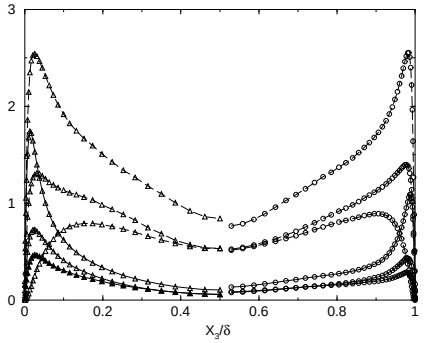

Figure 2: Subgrid and resolved stresses Δ: LES 1; $\circ$: LES 2. i=1,2,3 from top. SGS —; LES - -

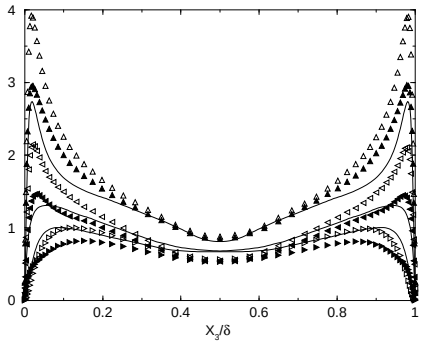

(a)

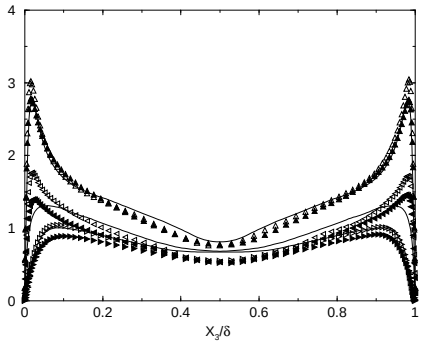

(b)

Figure 3: Turbulent Reynolds stresses $(\langle (\tau_{ii})_{sgs} \rangle + \langle (\tau_{ii})_{les} \rangle)^{\frac{1}{2}} / u_\tau$. (a), LES 1 ($16 \times 32 \times 64$). (b), LES 2 ($32 \times 64 \times 84$). LES : ▲: i=1; ◀: i=2; ▶: i=3; Smagorinsky : △: i=1; ◁: i=2; ▷: i=3; DNS :—; $R_\tau = 395$.

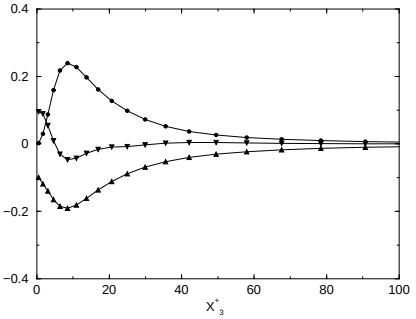

Figure 4: Terms in the budget equation of the subgrid energy. ● : $\nu P_{sgs}/u_\tau^4$; ▼ : $\nu J_{sgs}/u_\tau^4$; ▲ : $-\nu\epsilon_{sgs}/u_\tau^4$. (a), LES 1 ($16 \times 32 \times 64$).

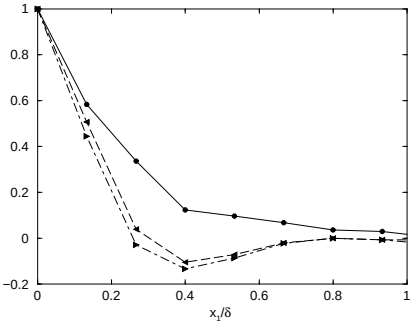

Figure 5: Streamwise two-point correlation function in the streamwise direction $\omega_1 \nu / u_\tau^2 = 0.04$. R_{11}; $--R_{22}$; $-.-R_{33}$. $x_3 = \delta$; (a), LES 1 ($16 \times 32 \times 64$).

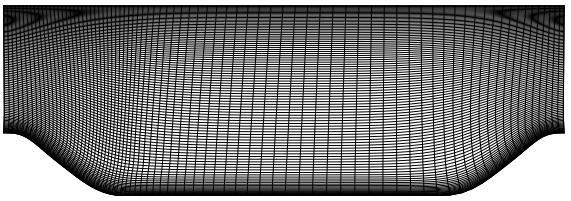

Figure 6: Cross-section of the curvilinear grid 80×100 of the contracted channel.

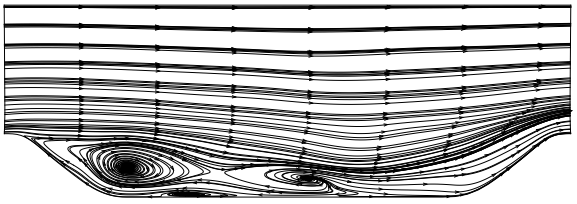

Figure 7: Streamlines of the instantaneous flow field predicted by LES (PITM) at $Re = 10595$

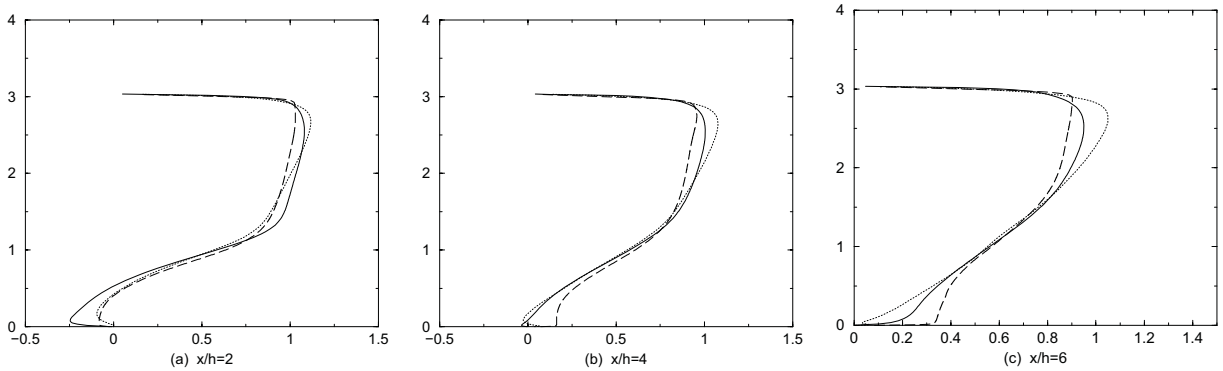

Fig 8. Streamwise velocity profiles $\langle U_1/U_b \rangle$ at $x/h = 2$, $x/h = 4$, $x/h = 6$ LES (Breuer et al., 2009) —; PITM $\cdots$; RSM - -.

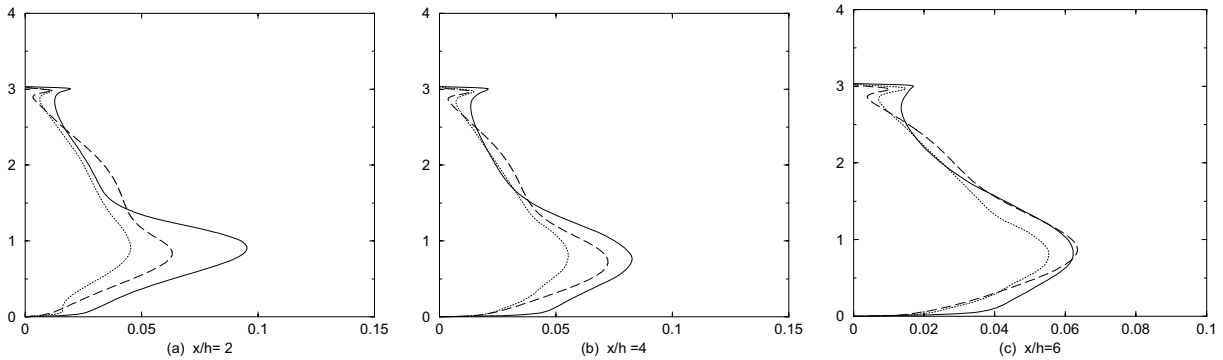

Fig 9. turbulent energy k/U_b^2 at $x/h = 2$, $x/h = 4$, $x/h = 6$. LES (Breuer et al., 2009) —; PITM $\cdots$; RSM - -.

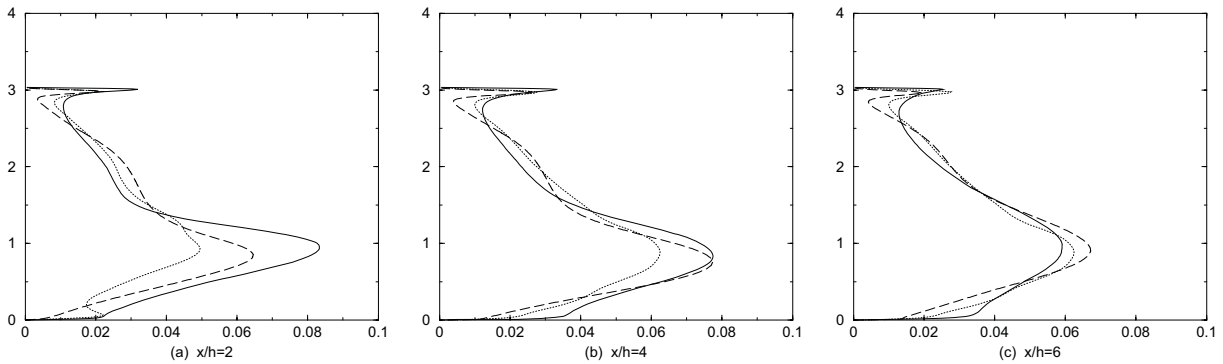

Fig 10. Streamwise turbulent energy τ_{11}/u_b^2 at $x/h = 2$, $x/h = 4$, $x/h = 6$. LES (Breuer et al., 2009) —; PITM $\cdots$; RSM - -.

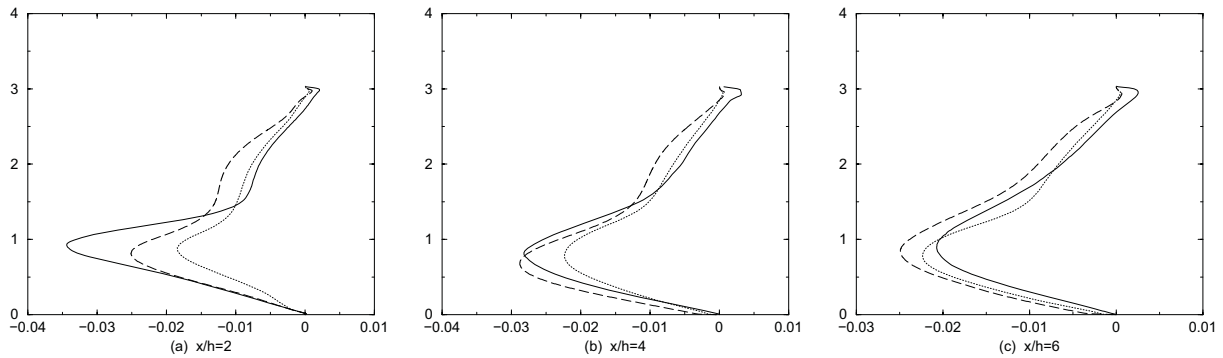

Fig 11. Turbulent shear stress τ_{13}/u_b^2 at $x/h = 2$, $x/h = 4$, $x/h = 6$. LES (Breuer et al., 2009) —; PITM $\cdots$; RSM - -.